NeuroImage 245 (2021) 118729

Contents lists available at ScienceDirect

NeuroImage

journal homepage: www.elsevier.com/locate/neuroimage

Emotion dysregulation and integration of emotion-related brain networks affect intraindividual change in ADHD severity throughout late adolescence

Tammo Viering[a,b,*], Pieter J. Hoekstra[b], Alexandra Philipsen[c], Jilly Naaijen[d,e], Andrea Dietrich[b], Catharina A. Hartman[f], Barbara Franke[g,h], Jan K. Buitelaar[d,e,i], Andrea Hildebrandt[j], Christiane M. Thiel[a,k,l], Carsten Gießing[a]

[a] Biological Psychology, Department of Psychology, School of Medicine and Health Sciences, Carl-von-Ossietzky Universität Oldenburg, Postfach 2503, Oldenburg 26111, Germany
[b] University of Groningen, University Medical Center Groningen, Department of Child and Adolescent Psychiatry, Groningen, Netherlands
[c] Department of Psychiatry and Psychotherapy, University of Bonn, Bonn, Germany
[d] Radboud University Medical Center, Donders Institute for Brain, Cognition and Behaviour, Department of Cognitive Neuroscience, Nijmegen, Netherlands
[e] Radboud University, Donders Institute for Brain, Cognition and Behaviour, Centre for Cognitive Neuroimaging, Nijmegen, Netherlands
[f] Department of Psychiatry, University of Groningen, University Medical Center Groningen, Interdisciplinary Center Psychopathology and Emotion Regulation, Groningen, Netherlands
[g] Radboud University Medical Center, Donders Institute for Brain, Cognition and Behaviour, Department of Human Genetics, Nijmegen, Netherlands
[h] Radboud University Medical Center, Donders Institute for Brain, Cognition and Behaviour, Department of Psychiatry, Nijmegen, Netherlands
[i] Karakter Child and Adolescent Psychiatry University Centre, Nijmegen, Netherlands
[j] Psychological Methods and Statistics, Department of Psychology, School of Medicine and Health Sciences, Carl-von-Ossietzky Universität Oldenburg, Oldenburg, Germany
[k] Research Center Neurosensory Science, Carl-von-Ossietzky Universität Oldenburg, Oldenburg, Germany
[l] Cluster of Excellence "Hearing4all", Carl von Ossietzky Universität Oldenburg, Oldenburg, Germany

ARTICLE INFO

Keywords:
Attention deficit/hyperactivity disorder
Emotion dysregulation
Latent change score modeling
Nodal efficiency
Orbitofrontal cortex
Resting state fmri

ABSTRACT

The course of attention deficit hyperactivity disorder (ADHD) from adolescence into adulthood shows large variations between individuals; nonetheless determinants of interindividual differences in the course are not well understood. A frequent problem in ADHD, associated with worse outcomes, is emotion dysregulation. We investigated whether emotion dysregulation and integration of emotion-related functional brain networks affect interindividual differences in ADHD severity change. ADHD severity and resting state neuroimaging data were measured in ADHD and unaffected individuals at two points during adolescence and young adulthood. Bivariate latent change score models were applied to investigate whether emotion dysregulation and network integration affect ADHD severity changes. Emotion dysregulation was gauged from questionnaire subscales for conduct problems, emotional problems and emotional lability. Better emotion regulation was associated with a better course of ADHD (104 participants, 44 females, age range: 12–27). Using graph analysis, we determined network integration of emotion-related functional brain networks. Network integration was measured by nodal efficiency, i.e., the average inverse path distance from one node to all other nodes. A pattern of low nodal efficiency of cortical regions associated with emotion processing and high nodal efficiency in subcortical areas and cortical areas involved in implicit emotion regulation predicted a better ADHD course. Larger nodal efficiency of the right orbitofrontal cortex was related to a better course of ADHD (99 participants, 42 females, age range: 10–29). We demonstrated that neural and behavioral covariates associated with emotion regulation affect the course of ADHD severity throughout adolescence and early adulthood beyond baseline effects of ADHD severity.

1. Introduction

The course of attention deficit/hyperactivity disorder (ADHD) in young adulthood differs strongly between individuals. While many individuals with ADHD show no or only mild symptoms in young adulthood, others show a high level of persistence (Biederman et al., 2011). Variables that account for interindividual differences in the development of ADHD are not well understood, but there is strong evidence that the ability to regulate emotions is one key factor of individual changes (Sudre et al., 2020). Whereas emotion processing refers to the process of assigning an emotional value towards a perceived stimulus, either positive or negative, emotion regulation describes starting, stopping, or modulating the trajectory of emotions to reach individual goals

* Corresponding author.
E-mail address: tammo.viering@uni-oldenburg.de (T. Viering).

https://doi.org/10.1016/j.neuroimage.2021.118729.
Received 13 April 2021; Received in revised form 11 November 2021; Accepted 13 November 2021
Available online 20 November 2021.

(Etkin et al., 2015). Dysregulation of emotion belongs to the most frequently observed co-occurring problems in ADHD (Shaw et al., 2014) and its presence in ADHD is associated with significant reductions in quality of life (Bunford et al., 2015; Riley et al., 2006; Wehmeier et al., 2010). The prevalence of ADHD decreases with age from approximately 11.4% in elementary school-aged children to 5.0% in young adults (Polanczyk et al., 2014; Willcutt, 2012). In contrast, the proportion of individuals with ADHD affected by emotion dysregulation increases from around 25–45% in childhood to 30–70% in young adulthood (Shaw et al., 2014). Clinical studies comparing categorical ADHD trajectories confirmed that emotion dysregulation, beside other variables like conduct problems, anxiety and depression, significantly relates to persistent ADHD (Caye et al., 2016; Sasser et al., 2016).

On neural level, several brain imaging studies support that ADHD is a heterogeneous disorder in which alterations are not limited to neural circuits of cognitive control. They also comprise structures associated with emotion processing and implicit (i.e., automatized and non-volitional) emotion regulation (Posner et al., 2014; Rubia, 2011) that is performed without conscious monitoring or awareness (e.g., inhibition of fear) (Etkin et al., 2015). Accordingly, altered functional connectivity in persons with ADHD is commonly found in the ventromedial prefrontal cortex, orbitofrontal cortex, frontal pole, amygdala, and ventral striatum (Bos et al., 2017; Costa Dias et al., 2013; Ho et al., 2015; Posner et al., 2013). Studies on ADHD using graph theory-based methods found alterations of brain network topology in medial and orbital prefrontal regions (Lin et al., 2014; L. Wang et al., 2009). In childhood ADHD, emotion dysregulation was shown to be correlated with functional connectivity of the amygdala, anterior cingulate, and insula (Hulvershorn et al., 2014; Yu et al., 2016). Moreover, task-based fMRI research using emotion perception and processing tasks in ADHD found evidence for abnormalities in the amygdala and insula (Brotman et al., 2010; Herpertz et al., 2008), while implicit emotion regulation in ADHD, investigated with fear extinction via habituation or emotional Stroop paradigms, was shown to be characterized by differences in the ventral anterior cingulate and ventromedial prefrontal cortex (Materna et al., 2019; Posner et al., 2011; Spencer et al., 2017). In summary, there is strong evidence that brain regions involved in emotion processing and implicit emotion regulation strongly deviate in subjects with ADHD. Following this line of evidence, we focused on functional brain network topology of brain regions involved in emotion processing and implicit emotion regulation rather than areas commonly associated with top-down processes of cognitive control.

Despite the strong evidence that brain regions involved in emotion processing differ in subjects with ADHD, little is known on the covariates that predict the course of ADHD. Previous studies compared neural activation between young adult groups with different categorical trajectories of prior ADHD diagnoses (e.g., remittent vs. persistent ADHD) (Shaw and Sudre, 2021). Those studies revealed that persistent ADHD is associated with atypical frontoparietal activity, i.e., activity of neural circuits associated with cognitive control (Francx et al., 2015; Schulz et al., 2017; Szekely et al., 2017). Structural abnormalities in cognitive control networks, but also in regions associated with emotion regulation were found to be associated with persistent ADHD (Shaw et al., 2013, 2015). By comparing individuals with different ADHD outcomes, it has been further shown that adults with persistent ADHD, but not remittent ADHD, exhibit abnormal functional connectivity in the default mode network, a network related to self-referential processing and emotion regulation (Mattfeld et al., 2014; Sudre et al., 2017). However, since most studies only examined brain activity at an adult age, they do not inform on whether respective differences existed previously (Mattfeld et al., 2014; Sudre et al., 2017). Hence, to our knowledge previous studies did not collect neural data at baseline to predict the course of ADHD. We here consider functional imaging data measured at baseline to examine how it affects interindividual differences in the change of ADHD severity. In contrast to previous studies, which categorically defined ADHD trajectory, we here investigated ADHD severity as continuous variable and modelled interindividual differences in the intraindividual change of ADHD to better gage individual changes.

Here, we examined the relationship of baseline emotion dysregulation and functional brain network topology of regions associated with emotion processing and implicit dysregulation with interindividual differences in the change of ADHD severity measured at two timepoints, in late adolescence and after about four years in early adulthood. Resting-state fMRI data was obtained at the same two time points as the ADHD severity information and analyzed using graph theory. Functional graphs were constructed considering functional connectivity of brain regions associated with both emotion dysregulation and ADHD. We focused on nodal efficiency, a parameter that describes how well a node is integrated within a network. Reduced efficiency (nodal as well as global) of functional brain networks has been associated with deficits in a wide variety of processes and is found in neurological, as well as psychiatric disorders (Achard and Bullmore, 2007; Cai et al., 2020; Ma et al., 2018; Rocca et al., 2016; Shim et al., 2018; Y. Wang et al., 2018). Deficits in efficiency were also related to emotion dysregulation and ADHD (Chen et al., 2019; Lin et al., 2014; Pan et al., 2018; L. Wang et al., 2009).

In order to analyze early indicators of later change in ADHD severity, we used latent change score models. As recently proposed, they allow modeling of the impact of continuous covariates on intraindividual changes during development (Kievit et al., 2018). In a first latent change score model, we investigated emotion-related and ADHD severity data aiming to explore whether emotion dysregulation predicts changes in ADHD severity approximately three to four years later. In a second model, using neural data, we assessed the efficiency of brain networks involved in emotion regulation and investigated possible underlying neural mechanisms of between–person differences in intraindividual ADHD courses. We hypothesized that both increased baseline emotion dysregulation and reduced baseline nodal efficiency of brain regions associated with emotion processing and emotion regulation negatively affect the course of ADHD.

2. Materials and methods

2.1. Participants and procedures

The present data were taken from NeuroIMAGE I and II, the second and third wave of an integrated-cognition-MRI-phenotype project on ADHD (von Rhein et al., 2015). No fMRI data were collected during the first wave, which was part of the International Multicenter ADHD Genetics study (IMAGE). Thus, data were taken from a well-established ADHD cohort. Previous studies investigating this data set already documented neural correlates of ADHD and associated problems like cognitive dysfunctions (Duan et al., 2018; Hoogman et al., 2019; Pruim et al., 2019). For instance, prior results suggest that cognitive dysfunctions (i.e., decreased working memory performance) in ADHD are mediated by inferior fronto-striato-cerebellar networks (Duan et al., 2018). In the following, the second and third wave are referred to as T1 and T2. Initially, individuals with combined presentation ADHD and unaffected individuals were recruited. For 244 individuals, phenotypical data was collected at both time points. A purely phenotypical analysis was performed on 104 (females: 44, average age at T1: 16.53, average age at T2: 20.09) of the 244 participants, for whom all required questionnaire data was available (Section 2.4). From 119 of the 244 participants, resting-state fMRI (rs-fMRI) data was acquired at T1 and T2. Of those 119 participants, 10 were excluded from rs-fMRI analysis due to left-handedness, as differences between left- and right-handed individuals exist in ADHD prevalence (Simões et al., 2017). Another 10 participants were excluded due to excessive movement in the scanner (root mean squared framewise displacement > 0.25). Thus, the current rs-fMRI analysis (Sections 2.3 and 2.4) was conducted on a sample of 99 individuals (females: 42, average age at T1: 17.22, average age at T2: 20.97). 58 individuals were

part of both the phenotypic and neuroimaging sample. Further sample characteristics are summarized in Section 3.1 and supplementary table S1.

All diagnostic and phenotypic data were acquired at the dates of the fMRI data collection. ADHD diagnoses were reassessed by combining information from the Kiddie Schedule for Affective Disorders (K-SADS) (Kaufman et al., 1997) and parent, teacher, and self-report versions of Conners' rating scale (CPRS-R:L, CTRS-R:L, & CAARS-R:L) (Conners et al., 1999; Conners et al., 1998a, 1998b). A combined symptom count derived from the K-SADS and the different versions of Conners' rating scale (von Rhein et al., 2015) was used as an indicator for ADHD severity. Here, the CTRS-R:L was used for individuals under 18 years of age, while the CAARS-S:L was used for individuals over 18. K-SADS and Conners' rating scales provide DSM-IV-based definitions of ADHD symptoms. If a symptom was present in at least one of them, it counted towards the final symptom sum score with one point. Emotion dysregulation was gauged as a linear combination of three questionnaire subscales. These subscales are the emotional lability subscale of CPRS-R:L (three items for unpredictable mood changes, temper tantrums, and tearfulness) and the emotional problem (five items for anxieties, worries, happiness, and physical symptoms of emotional stress) and conduct problem (five items for temper tantrums, compliance, quarrelsomeness, stealing, and lying) subscales of the Strengths and Difficulties Questionnaire (SDQ) (van Widenfelt, Goedhart, Treffers, and Goodman, 2003). For a detailed description of the diagnostic procedures, the creation of the combined symptom counts and the initial recruitment we refer to Rhein et al. (2015).

Forty-eight hours prior to testing, stimulant medication use was discontinued. Data acquisition took place at the Donders Institute for Cognitive Neuroimaging, Radboud University Nijmegen, Netherlands. Participants (and their parents when <18 years old) gave written informed consent for participation. Ethical approval was granted by the regional ethics board (Centrale Commissie Mensgebonden Onderzoek: CMO Regio Arnhem Nijmegen, ABR: NL41950.091.12). The data is stored in the Donders Institute for Cognitive Neuroimaging and may be requested via the corresponding author.

2.2. Resting-state fMRI data acquisition and preprocessing

Identical scanning protocols were used for NeuroIMAGE I and II. Imaging was performed on a 1.5 T Magnetom Avanto (Siemens AG, Erlangen, Germany). BOLD-sensitive resting-state functional volumes were acquired using a T2*-weighted EPI sequence (TR=1960 ms, TE=40 ms). Each of the 266 vol consisted of 37 axial slices of size 64×64 (flip angle = 80°, FoV = 224×224 mm2, voxel-size = 3.5 × 3.5 × 3.0 mm3, inter-slice gap = 0.5 mm). T1-weighted high-resolution structural volumes were acquired with an MPRAGE sequence (TR = 2730 ms, TE = 2.95 ms, TI = 900 ms, flip angle = 9°, FoV = 256×256 mm2, voxel- size = 1.0 × 1.0 × 1,0 mm3, GRAPPA 2). Root mean squared framewise displacement was calculated (mean=0.071, SD=0.040). A threshold of 0.25 was applied to exclude 10 participants with extreme movement at either T1 or T2 from further analysis. Using a linear mixed effects model with subjects as random effects, it was tested whether root mean squared framewise displacement significantly depends on age, nodal efficiency measures (principal component scores) or the diagnostic status. Type II/III Wald F-tests were conducted. None of the investigated variables showed a significant impact (age: $F(1, 156.69) = 0.074$, $p = 0.787$; diagnosis(categorical): $F(2, 146.03) = 1.085$, $p = .341$; nodal efficiency: $F(1, 191.85) = 1.632$, $p = .203$). We therefore assume that to a large extent motion effects did not influence the results of our analysis to a large extent.

Preprocessing was mainly conducted using FSL FMRIB algorithms (FSL 5.0.11) (Jenkinson et al., 2012). After dropping the first five scans of the resting-state time series, the images were skull stripped, realigned to the middle volume of the series, and co-registered to the structural T1. ICA-AROMA was applied to account for motion artefacts (Pruim et al., 2015). In addition, nuisance signal was reduced by regressing out the average BOLD time courses of the white matter and cerebrospinal fluid, and the linear trend. High-pass filtering was conducted at 0.01 Hz. Finally, the data was warped into MNI152 space (Montreal Neurological Institute, Montreal, Canada).

2.3. Graph analysis

Python 3.5 with NetworkX (Hagberg et al., 2008) was used for graph analysis. Parcellation of preprocessed time series data was realized using a hemisphere-specific functional brain template with 268 parcels (Finn et al., 2015; Shen et al., 2013). This atlas was chosen as it was created using a graph-theoretically based parcellation approach that ensures functional homogeneity within the parcels of the atlas. To ensure that the analysis yields similar results regardless of the parcellation scheme selected, the analysis described below was additionally performed using an alternative brain template with 246 functionally homogenous nodes (Fan et al., 2016).

Emotion network extraction. The current study aimed to relate changes in ADHD severity with network integration of brain nodes involved in emotion dysregulation. Hence, 48 parcels of the selected template were chosen that overlapped with the orbitofrontal cortex, ventromedial prefrontal cortex, anterior cingulate cortex, insula, ventral striatum, amygdala, and hippocampus as defined by the Harvard-Oxford Brain Atlas by more than 30%. These brain regions have been previously shown to be involved in emotion processing, its implicit regulation, and brain dysfunctions in ADHD (Materna et al., 2019; Rubia, 2018; Shaw et al., 2014). The focus here is not on structures that achieve emotion regulation via cognitive control and reappraisal (e.g., frontostriatal network), but rather on those that are related to emotion processing and implicit emotion regulation (Etkin et al., 2015). All subsequent rs-fMRI analyses including the calculation of nodal efficiency measures described below were performed on the functional connectivity of these 48 nodes.

Graph construction. Subject-specific average BOLD time series were calculated for each of the 48 parcels. Correlation matrices were created by computing pairwise Pearson's correlations between the extracted time series. The matrices were Fisher's *Z*-transformed and transformed into absolute values as negative correlations are also thought to be functionally relevant (Hallquist and Hillary, 2019). Due to the relatively low number of negative correlations (22.1% of all edges), we refrained from performing specific analysis for positive and negative correlations. To distinguish differences in network density from those of network topology (Ginestet et al., 2011), the matrices were binarized based on eight equally spaced density thresholds with a minimum density of 0.10 and a maximum density of 0.45 (Achard and Bullmore, 2007). In this range of low to medium network densities, previous studies found significant associations between network topology and ADHD symptoms (Lin et al., 2014; L. Wang et al., 2009). Thus, for each of the binarized matrices a density-specific network graph was created. A detailed discussion of the advantages and disadvantages of density-based thresholds can be found in van Heuvel et al. (2017).

Analysis of nodal integration. Nodal efficiency is a measure related to the average number of edges that must be traversed to connect a given node to all other nodes of the network. Nodes with high nodal efficiency need few edges to connect with other nodes and easily propagate information to other nodes in the network. Brain network efficiency is associated with a wide range of neural processes, such as cognition and emotion regulation, as well as neurological and psychiatric disorders, especially ADHD (L. Wang et al., 2009). The current analysis focused on a set of selected brain nodes to investigate whether differences in the integration and the formation of the emotional subnetwork affects the individual ADHD severity. A summary of the functional connectivity and network analysis is provided by the supplementary Figure S1.

2.4. Statistical analysis and bivariate latent change score models

Overview. By means of a bivariate latent change score (BLCS) model with phenotypical data, we investigated whether emotion dysregulation at T1 is related to change in ADHD severity from T1 to T2. Within this model, the relationships of change in emotion dysregulation from T1 to T2 with ADHD severity at T1 and change in ADHD severity were also estimated. By applying a BLCS model on neuroimaging data, we further investigated whether the integration of nodes linked to emotion processing and implicit regulation, i.e. nodal efficiency, at T1 predicts change in ADHD severity from T1 to T2. Within these models, the relationships of change in nodal efficiency from T1 to T2 with ADHD severity at T1 and change in ADHD severity were also estimated. Due to the small number of participants with complete phenotypical and neuroimaging data, we refrained from using one model that includes rs-fMRI as well as emotion-related data.

Advantages of bivariate latent change score. BLCS analyses were performed by using the **R** Software for Statistical Computing (Team and R Development Core Team, 2016) and the lavaan library (Rosseel, 2012). These models are a powerful and flexible class of structural equation models (SEM) which allow testing a wide range of developmental hypotheses (Kievit et al., 2018). For two variables that are measured at two different points in time, the change of the variable across time is estimated as a latent change score. The variables for which change score are modeled may themselves be latent, thus, reflected by a set of measured variables. In contrast to cross-sectional comparisons or other longitudinal modeling approaches, BLCS models allow estimating parameters that capture the extent to which the change between time points depends on baseline values and other not directly observable, latent variables (Kievit et al., 2018). For example, we can capture the extent to which changes in ADHD severity are a function of ADHD severity at baseline, and also of latent emotion dysregulation scores or nodal efficiency at T1. While not directly revealing causal relations, BLCS models may be used to test model-based predictions of causal hypotheses (Kievit et al., 2018).

Robustness of the approach. Prior to model generation and parameter estimation, the measured variables were checked for multivariate normality using Mardia's multivariate skewness and kurtosis coefficients (Mardia, 1970) and outliers using Mahalanobis' distance. Mahalanobis' distance measures typically follow a χ^2-distribution. Consistent for both BLCS approaches, an outlier exclusion threshold of $p > .001$ was applied to exclude individuals with extreme behavioral or neural data (see below for further explanations). In order to further minimize the influence of potential outliers and violations of multivariate normality, a robust maximum likelihood estimator was used for SEM (Yuan and Zhong, 2013). Thus, several attempts were made to secure the robustness of the results.

Significance testing and further indices of model quality. The significance of SEM parameter estimates was assessed by the Wald-test statistic. Regression coefficient estimates relevant for the research question were additionally tested by means of a χ^2-difference test. To this end, nested BLCS models were compared in which the respective regression parameter was freely estimated vs. fixed to zero. The regression and intercept parameters estimated within the BLCS model are partial coefficients, implying that influences of other modeled variables are accounted for. Individuals with missing values were not included in any analysis. Standardized parameter estimates are reported.

Whenever appropriate, goodness of fit measures, namely the comparative fit index (CFI), standardized root mean square residual (SRMR), and root mean square error of approximation (RMSEA) are reported. Acceptable goodness-of-fit measures should at least be above 0.95 for the CFI, below 0.08 for the SRMR, and below 0.10 for the RMSEA (Schermelleh-Engel et al., 2003).

2.4.1. BLCS model with emotion dysregulation data

See Fig. 1A for a path diagram of the applied BLCS model. The aim of the first analysis was to investigate the relationships of ADHD severity and emotion dysregulation at T1 with changes in emotion dysregulation and ADHD severity from T1 to T2. The model additionally provides parameter estimates indicating the relationship between the change scores.

The BLCS model included latent variables describing emotion dysregulation at T1 and T2. These latent variables were derived from three aforementioned questionnaire subscales of emotional lability, emotional problems, and conduct symptoms. Thus, emotional dysregulation at T1 and T2 was estimated as latent variable summarizing the three phenotypical scales. For the latent emotion dysregulation scores as well as for ADHD severity latent change scores were estimated. They capture the average change of the respective variables from T1 to T2 and the variance of change across individuals.

Severity of ADHD at T2 was modelled by the sum of ADHD severity at T1 and the change in ADHD severity from T1 to T2. Emotion dysregulation at T2 was modelled according to the same principle. The model provides covariance estimates between ADHD severity and emotion dysregulation at T1. Likewise, the covariance between the two change score variables was estimated as well. Factor loadings onto the latent emotion dysregulation variable were assumed to be invariant across time and thus fixed to equality. To account for the shared method variance due to measurement repetitions, residual covariances were allowed over time.

2.4.2. BLCS model with functional brain network data

See Fig. 2B for the path diagram illustrating the BLCS model including the neural data. The aim of the second analysis step was to investigate the relationship of ADHD severity and nodal efficiency at T1 with the change in nodal efficiency and ADHD severity from T1 to T2. The models also estimated the relationship between the changes scores.

Cost-integrated nodal efficiency (see 2.3) was investigated in two separate BLCS analyses. Both analyses addressed the relationship of nodal efficiency in emotional brain networks with ADHD severity across two points in time. The first analysis was performed on node-integrated values summarizing nodal efficiency information from all 48 nodes. Principal component analyses (PCA) were separately computed for time point T1 and T2 to integrate nodal efficiency of each individual subject across the 48 brain nodes The first PC score, which is a linear combination of nodal efficiency from all 48 nodes was modeled in BLCS. We focused on the first PC considering it to be a low dimensional and robust summary of individual nodal efficiency that reflect the maximum variability between individuals. Thus, the PC scores were entered into a BLCS model to assess possible relationships between ADHD severity and an integrated estimate summarizing nodal efficiency of the network associated with emotion processing and implicit emotion regulation. The second analysis only used node-specific information. 48 different models were estimated, each for one node only. Alpha inflation due to multiple comparison was controlled by the Benjamini-Hochberg false-discovery (FDR) procedure (Benjamini and Hochberg, 1995).

For both analyses, latent change scores were created for ADHD severity and the nodal efficiency variables. Severity of ADHD at T2 was modelled by the sum of ADHD severity at T1 and the change in ADHD severity from T1 to T2. Nodal efficiency at T2 was modelled following the same principle. The covariance between ADHD severity and the latent emotional problems variable was estimated as well. Likewise, the covariance between the two change score variables was specified.

2.4.3. Additional analyses

Correlation analyses were conducted to investigate whether nodal efficiency and the associated first PCs are related with the latent emotion dysregulation variable derived from questionnaire data. Individual factor scores for the latent variables were obtained using factor score regression with the lavPredict-function of lavaan (Devlieger et al., 2016). Using analysis of variance (ANOVA), we additionally investigated the impact of medication status on the change in ADHD severity. Participants were divided into four groups. The first group consisted of those who took stimulant medication during T1 and T2, group two and three

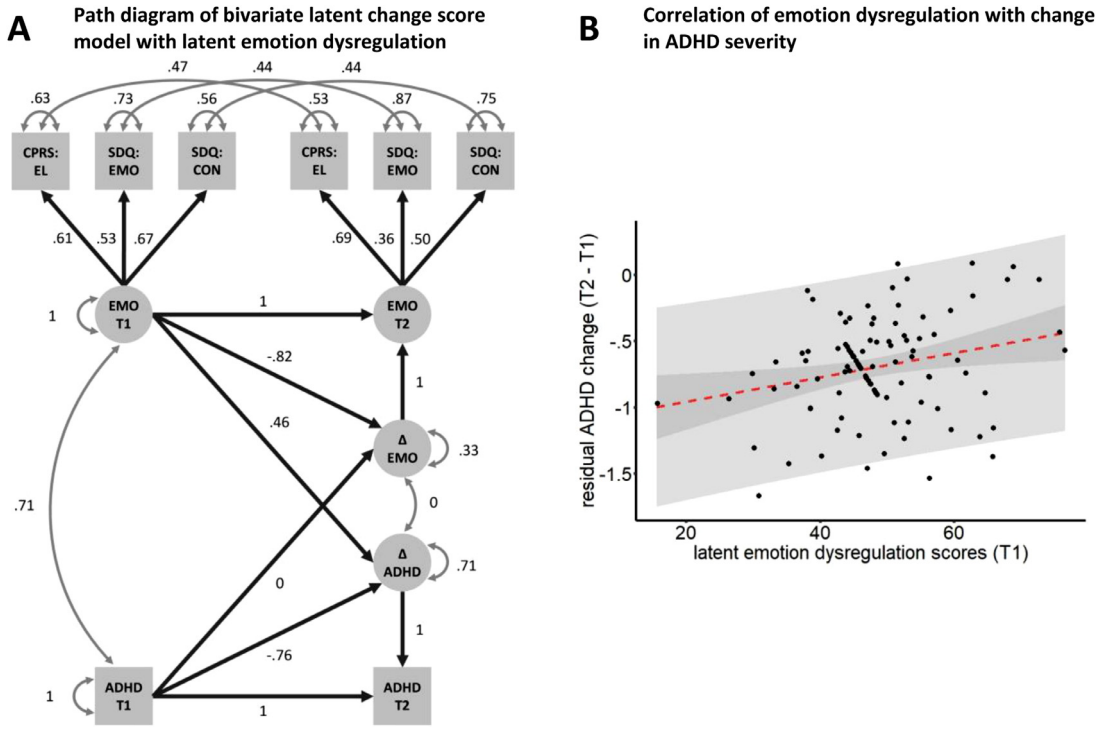

Fig. 1. Results of bivariate latent change score analysis with latent emotion dysregulation scores. **[A] Path diagram of bivariate latent change score model with latent emotion dysregulation:** Standardized parameter estimates are included as path coefficients (regression weights). Non-significant parameters were set to zero. Results of the phenotypical analysis using latent emotion dysregulation scores are displayed. **[B] Correlation of emotion dysregulation with change in ADHD severity:** A scatter plot with the linear fit was created for emotion dysregulation at T1 and individual change in ADHD severity from T1 to T2. The dark gray area indicates 95%-*confidence* intervals. The light gray area indicates 95%-*prediction* intervals. The points forming a line represent those individuals that received an ADHD severity score of zero at T1 and T2 and whose estimated change was derived solely from their emotion dysregulation scores at T1 (n = 23).

of those who took stimulant medication at T1 or T2, and the final group of those who did not take stimulant medication at any time.

3. Results

3.1. Sample characteristics

Participants were on average 17.22 years old at T1 and 20.97 years at T2. On average, the time period between T1 and T2 was 3.75 years (SD = 0.503, Range = 2.64–5.18). Using the Wilcoxon signed rank test, a significant decrease was observed for ADHD hyperactivity-impulsivity symptoms scores (W = 1401.5, p = .006, r = 0.344). Average IQ increased significantly ($t(97)$=−2.370, p = .020) and significant changes in the use of stimulants were observed (χ^2 = 12.042, p < .001). All other relevant variables remained constant. Demographic details of the sample are summarized in Table 1. Sample characteristics as a function of subgroup can be found in figure S2 and table S1 of the Supplement.

3.2. BLCS model with emotion dysregulation data

We first investigated whether emotion dysregulation at T1 is associated with change in ADHD severity. Prior to model estimation, one participant was identified as outlier and discarded due to large Mahalanobis' distance.

Confirmatory factor analysis was conducted for initial variable selection. Significant loadings (fixed to be invariant across time points) were found for the emotional lability subscale of CPRS-R:L, (z = 4.356, p < .001, λ = 0.521), SDQ's emotional symptoms subscale (z = 3.342, p = .001, λ = 0.515), and SDQ's conduct symptoms subscale (z = 3.436, p = .001, λ = 0.485). Thus, all variables were considered for the BLCS model.

The BLCS model revealed a significant relationship of the latent emotion dysregulation at T1 with change in ADHD severity (z = 2.117, p = .034, β = 0.456; χ^2-difference-test: χ^2=5.545, p = .019). Higher emotion dysregulation at T1 was associated with less favorable change (smaller decrease of symptoms) in ADHD severity from T1 to T2. The relationship of ADHD severity at T1 with change in emotion dysregulation and the relationship of the changes were not significant. Respective parameters were set to zero for the final parameter estimation. The final BLCS model ($\chi^2(17)$ = 22.257, p = .175) provided satisfactory goodness-of-fit (CFI = 0.987, SRMR = 0.047, RMSEA = 0.055). Fig. 1 summarizes the results of the BLCS model with phenotypical data.

3.3. BLCS model with functional brain network data

3.3.1. Whole-network BLCS analysis with nodal efficiencies after PCA

To investigate whether nodal efficiency of the emotion-related network was related to change in ADHD severity, a whole-network BLCS model was used such that nodal efficiency was combined across the emotion-related network using PCA. Nodes of the dorsal anterior cingulate cortex and insula were found to contribute negatively to the first PC and nodes of the basal ganglia, medial prefrontal cortex, orbitofrontal cortex, and hippocampus contributed positively (see Fig. 2C). The first PC captured 20.6% of the variance. Using Mahalanobis' distances and an alpha-threshold of 0.001, three participants were identified as outliers and discarded from the analysis.

The whole-network BLCS model revealed a significant relationship between the first PC at T1 and change in ADHD severity (z = −2.207, p = .027, β = −0.192; χ^2-difference-test: χ^2 = 5.1383, p = .023). The higher the PC scores at T1 were, the better was the change in ADHD severity from T1 to T2 (larger decreases of symptoms). The relationship of ADHD severity at T1 with change in the PC and the relationship of the changes were not significant. Respective parameters were

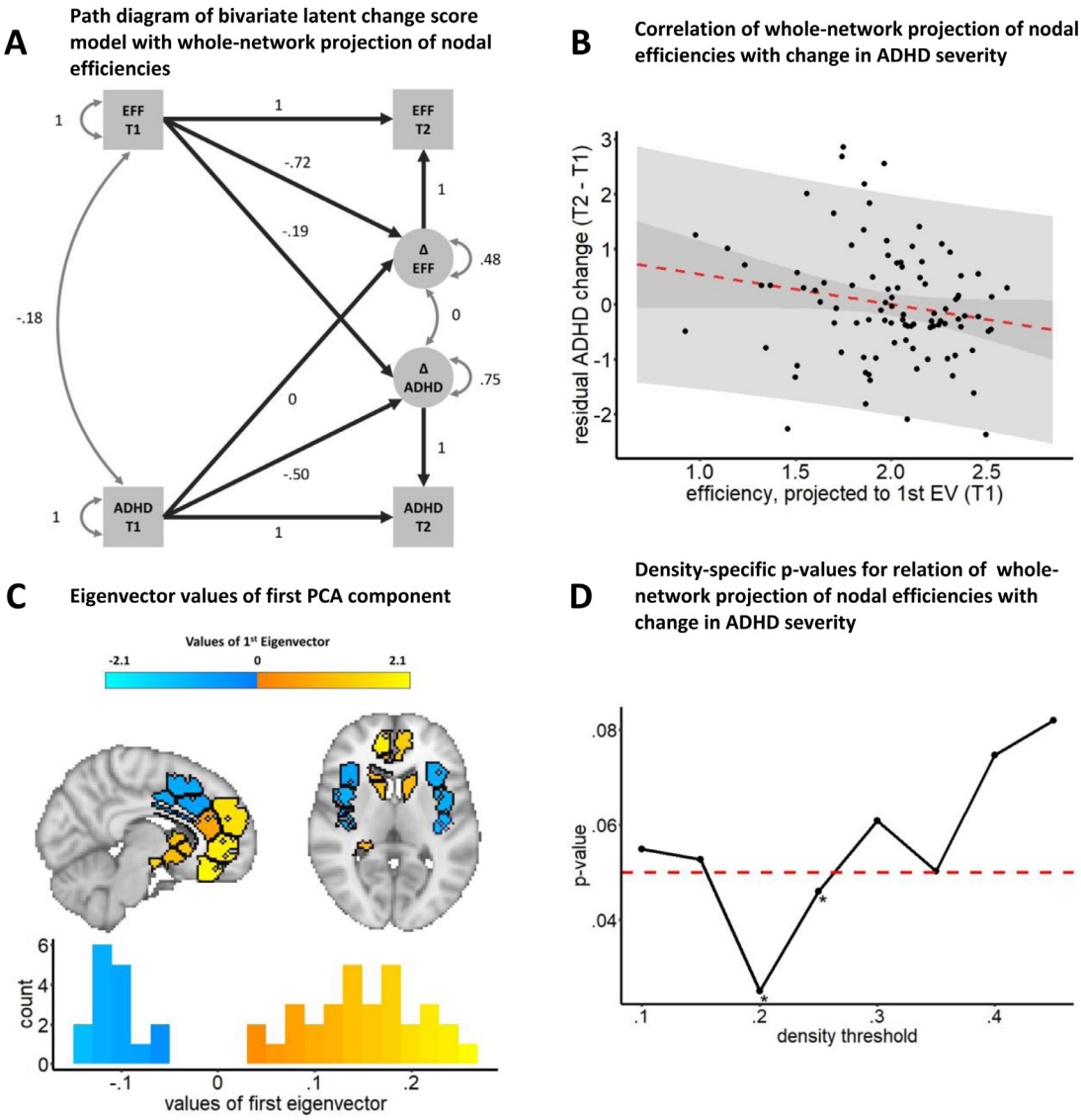

Fig. 2. Results of bivariate latent change score analysis with nodal efficiency of the whole emotional network summarized by their first principal component. **[A] Path diagram of significant bivariate latent change score model with whole-network projection of nodal efficiencies**: Standardized parameter estimates are included as path coefficients (regression weights). Non-significant parameters were set to zero. Results of the whole-network analysis with nodal efficiencies after principal component analysis are presented. **[B] Correlation of whole-network projection of nodal efficiencies with change in ADHD severity:** A scatter plot with the linear fit was created for the first PC at T1 and individual change in ADHD severity from T1 to T2. The dark gray area indicates 95%-*confidence* intervals. The light gray area indicates 95%-*prediction* intervals. **[C] Eigenvector values of first PCA component:** The values of the first eigenvector are associated with specific brain parcels. They reflect how strongly each node contributes to the first PCA component. The higher the absolute eigenvector value of a node, the more it contributes to the first PCA component. Dorsal anterior cingulate cortex and insula nodes were found to contribute negatively to the first PC while nodes of the basal ganglia, medial prefrontal cortex, orbitofrontal cortex, and hippocampus contributed positively. **[D] Density-specific p-values for relation of whole-network projection of nodal efficiencies with change in ADHD severity:** Density-specific p-values were calculated. The relation of the first PCA component at T1 with change in ADHD severity was investigated. χ^2-difference tests were used to obtain p-values. At each density-level an individual BLCS model was estimated.

set to zero for the final parameter estimation. The final BLCS model ($\chi^2(2) = 0.857, p = .651$) provided satisfactory goodness-of-fit measures (CFI = 1, SRMR = 0.023, RMSEA = 0). The analysis was repeated using density-specific nodal efficiency. The significant relationship of the first PC at T1 with change in ADHD severity, shown for density-integrated nodal efficiency, was confirmed with density thresholds 0.2 and 0.25 (see Fig. 2D). Fig. 2 summarizes the results of the BLCS model with network data after PCA.

3.3.2. Node-specific BLCS analysis

We used 48 BLCS models with node-specific efficiency to investigate the relationship of nodal efficiency of brain regions associated with emotion processing and implicit emotion regulation with change in ADHD severity. Mahalanobis' distances for the measured variables were calculated for all 48 BLCS models to identify outliers. Multivariate normality was evaluated separately for each model.

A significant relationship between nodal efficiency at T1 and change in ADHD severity was detected for the right orbitofrontal cortex ($z = -3.972$, $p = .003$ (BH-corrected), $\beta = -0.272$; χ^2-difference-test: $\chi^2 = 12.547$, $p = .019$ (BH-corrected for multiple comparisons)). The higher the nodal efficiency values at T1 were, the better were the changes in ADHD severity from T1 to T2 (larger decreases of symptoms). Parameter estimation of the associated BLCS model was conducted after exclusion of one outlier. The relationship of ADHD severity at T1 with change in nodal efficiency and the relationship of the changes were not significant. Respective parameters were set to zero for

Table 1
Characteristics of the resting-state fMRI sample at both data collection phases (T1 and T2).

$N = 99$	NeuroIMAGE I (T1)		NeuroIMAGE II (T2)		Difference test between T1 and T2		
	Mean	*SD*	*Mean*	*SD*	Test statistic	p-value	Effect-size
ADHD,hyperactivity-impulsivity symptoms	2.88	2.83	2.55	2.54	$W = 1401.5$	.006	$r = 0.34$
ADHD, inattention symptoms	3.68	3.24	3.05	3.01	$W = 1476$	.167	$r = 0.014$
age (years)	17.22	3.15	20.97	3.09	$t = -74.04$	< 0.001	$\delta = 7.44$
IQ (WISC/WAIS)	102.93	14.74	105.43	17.80	$t = -2.37$	.020	$\delta = 0.24$
CPRS-R:L emotional lability*	47.91	9.37	45.88	5.09	$W = 487.5$	.091	$r = 0.28$
SDQ emotional symptoms**	2.14	1.87	2.41	2.00	$W = 425$	.288	$r = 0.16$
SDQ conduct symptoms**	1.37	1.29	1.44	1.33	$W = 376.5$	.286	$r = 0.18$
	count		*count*				
Females	42		42				
individuals with ADHD-related impairments	51		45		$\chi^2 = 2.50$	.114	$g = 0.30$
Stimulant users	35		18		$\chi^2 = 12.04$	<0.001	$g = 0.38$
DSM-IV MDD (K-SADS)***	2		1		$\chi^2 = 0.50$	.480	$g = 0.50$
DSM-IV anxiety (K-SADS)***	6		3		$\chi^2 = 1.33$	.248	$g = 0.50$
DSM-IV ODD (K-SADS)***	12		6		$\chi^2 = 2.08$	.149	$g = 0.25$
DSM-IV CD (K-SADS)***	2		1		$\chi^2 = 0$	1	$g = 0.17$

Notes: Means between time points were either compared with paired-sample *t*-tests or Wilcoxon signed rank tests. Frequency distributions were compared using McNemar's test. For the CPRS-R: L *t*-scores are presented, while for the SDQ questionnaire scores are given. Cohen's δ or Cohen's g were used for effect sizes.; **ADHD** = Attention Deficit/Hyperactivity Disorder; **CD** = Conduct Disorder; **CPRS-R:L** = Conners' parent rating scale, revised, long version; **IQ** = Intelligence Quotient; **K-SADS** = Kiddie Schedule for Affective Disorders and Schizophrenia; ***MDD*** = major depressive disorder; ***N*** = number of participants; **ODD** = Oppositional Defiant Disorder; **CD** = Conduct Disorder; **SD** = standard deviation; **SDQ** = Strengths and Difficulties Questionnaire; ***t*** = test statistic for t-tests; ***W*** = test statistic for Wilcoxon signed rank test.
*data was available for 78 participants at T1 and 80 participants at T2.
**data was available for 59 participants at T1 and 80 participants at T2.
***individuals diagnosed with respective disorder.

the final parameter estimation. The final BLCS model ($\chi^2(2) = 1.827$, $p = .401$) provided satisfactory goodness-of-fit measures (CFI = 1, SRMR = 0.035, RMSEA = 0). The analysis was repeated using density-specific nodal efficiency. The significant relationship of nodal efficiency at T1 with change in ADHD severity, shown for density-integrated nodal efficiency, was confirmed with four density thresholds between 0.3 and 0.45 (see Fig. 3D). None of the other nodal BLCS models revealed a significant relationship between nodal efficiency and change in ADHD severity.

3.3.3. Additional analyses

Correlation analysis of nodal efficiency and emotion dysregulation at T1. To investigate whether baseline nodal efficiencies and emotion dysregulation are related, a correlation analysis was conducted. Emotion-related questionnaire subscales and rs-fMRI data were available for $N = 58$ participants. Using their latent emotion dysregulation scores at T1, it was shown that no significant correlations exist with node-integrated nodal efficiency ($r = 0.165$, $t(56) = 1.252$, $p = .215$) and nodal efficiency of the right orbitofrontal cortex ($r = 0.136$, $t(56) = 1.027$, $p = .309$) at T1.

BLCS analyses with alternative parcellation scheme. To show the robustness of our results, the BLCS analyses described above were repeated using an alternative parcellation scheme. The general pattern of results corresponded to that of the analyses using the primary parcellation scheme. In agreement with the previous analysis, a significant relationship of nodal efficiency of the right orbitofrontal cortex at T1 and change in ADHD severity was shown at a density threshold of 0.35 ($z = 3.316$, $p = .049$ (BH-corr.), $\beta = -0.277$). At the integrated level, however, the results did not remain significant after FDR correction ($z = 3.149$, $p = .265$ (BH-corr.), $\beta = -0.263$).

ANOVA for impact of medication status on ADHD severity scores. We used ANOVA to investigate if the medication status influences the change in ADHD severity scores. The change in ADHD severity did not significantly depend on the medication status at T1 and T2 ($F(3,94) = 1.893$, $p = .136$).

4. Discussion

We examined whether emotion dysregulation and nodal efficiency of brain regions associated with emotion processing and implicit emotion regulation, both measured during late adolescence, predicted change in ADHD severity across a period of three to four years. To this end, BLCS models were used to analyze the influence of nodal efficiency, derived using graph theory methods, and questionnaire data on emotional problems, conduct problems and emotional lability. At the symptom level, lower baseline emotion dysregulation was associated with more favorable change in ADHD severity. At the neural level, nodal efficiency integrated across emotion-related brain regions predicted changes in ADHD severity. Especially higher nodal efficiency in the area of the right orbitofrontal cortex was associated with more favorable course of ADHD. Baseline nodal efficiency and emotion dysregulation were however not significantly correlated.

It was previously shown that conduct problems, emotional problems and emotion dysregulation during childhood may be related to the course of ADHD (Biederman et al., 2011; Caye et al., 2016; Miranda et al., 2015). We add to this knowledge by showing that a latent variable derived from these variables, here referred to as emotion dysregulation, affects the course of ADHD severity from late adolescence to early adulthood. The results join a body of research that identified a clear link between emotion dysregulation and ADHD, specifically relating emotional and associated problems to the outcome of ADHD. Previous studies showed that individuals with emotional comorbidities and problems are often those with worse ADHD outcomes later in life (Biederman et al., 2011; Caye et al., 2016; Miranda et al., 2015; Sasser et al., 2016). Our findings, however, differ from most others in that we did not consider childhood ADHD, but ADHD in later stages of life, i.e., late adolescence and early adulthood. Also, rather than merely examining cross-sectional data or categorical outcome variables (e.g., persistent or remittent ADHD), we examined change and its dependence on emotion dysregulation through the use of latent change score models. In contrast to models that analyze aggregated data, these models can capture change at the individual level and detect differences in intrain-

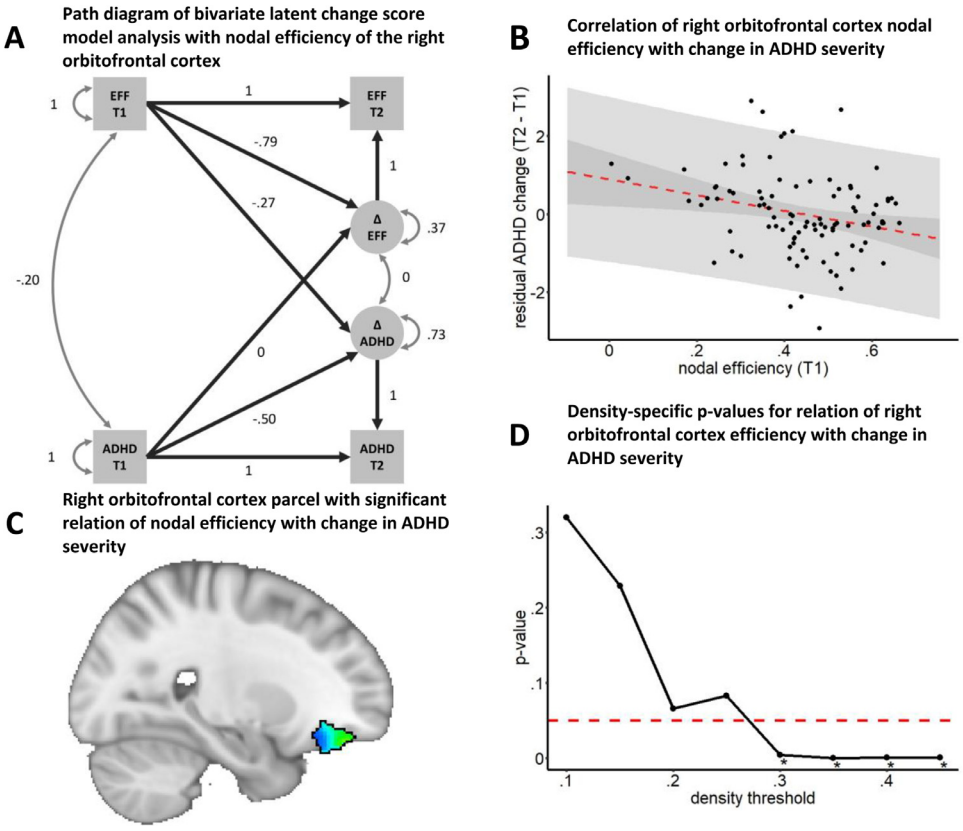

Fig. 3. Results of bivariate latent change score analysis with nodal efficiency of right orbitofrontal cortex. **[A] Path diagram of bivariate latent change score model analysis with nodal efficiency of the right orbitofrontal cortex:** Standardized parameter estimates are included as path coefficients (regression weights). Non-significant parameters were set to zero. **[B] Correlation of right orbitofrontal cortex nodal efficiency with change in ADHD severity:** A scatter plot with the linear fit was created for nodal efficiency of the right orbitofrontal cortex at T1 and individual change in ADHD severity from T1 to T2. The dark gray area indicates 95%-confidence intervals. The light gray area indicates 95%-prediction intervals. **[C] Right orbitofrontal cortex parcel with significant relation of nodal efficiency with change in ADHD severity:** Right orbitofrontal cortex nodal efficiency at T1 affected change in ADHD severity from T1 to T2. **[D] Density-specific p-values for relation of right orbitofrontal cortex efficiency with change in ADHD severity:** Density-specific *p*-values were calculated after applying FDR-procedures. The relation of nodal efficiency at T1 with change in ADHD severity from T1 to T2 was investigated. χ^2-difference tests were used to obtain *p*-values. At each density-level an individual BLCS models were estimated.

dividual changes (Baltes et al., 1988). Our results suggest that emotion dysregulation predicts the development of ADHD severity independent from ADHD severity at baseline and therefore may have clinical relevance.

The principal component analysis with nodal efficiencies of the whole network revealed that brain regions contributed differently to the first principal component. Cortical brain regions associated with emotion processing, e.g., the dorsolateral anterior cingulate cortex and the insula, contributed negatively, whereas regions associated with implicit emotion regulation, e.g., the medial prefrontal and orbitofrontal cortex, contributed positively (cf. Etkin et al., 2015). In agreement with our original hypothesis (compare Section 1), this pattern of opposed loadings indeed suggested that the investigated brain regions compose two anti-correlated, functionally separated subnetworks (emotion processing versus regulation). This clear separation on the cortical level was, however, not found on the subcortical level. Amygdala, striatum and parts of the brainstem, i.e., regions highly associated with fundamental emotional processes, showed positive loading. While subcortical structures extract rather simple emotional and motivational features, the insula provides additional interoceptive information (Uddin et al., 2017). The anterior cingulate cortex relates the emotional content to other emotional information (Etkin et al., 2015).

In summary, high individual scores in the first principal component were thus characterized by low nodal efficiencies in cortical regions of emotion processing and high nodal efficiencies in cortical regions of implicit emotion regulation, i.e., large differences in nodal efficiencies between these two subnetworks. The first principal component was found to predict the course of ADHD severity from late adolescence into early adulthood over and above baseline effects of ADHD severity. Thus, a pattern of low nodal efficiency within cortical structures associated with emotion processing and of high nodal efficiency within subcortical structures and cortical structures involved in implicit regulation may have a positive impact on the future course of ADHD. The results of the principal component-based analysis of the whole network support the view that, in ADHD, circuits related to emotion processing and implicit emotion regulation are relevant in addition to circuits associated with cognitive control and attention. They thus fit into a large body of literature that points to the importance of the regions studied in the present network analyses. For instance, ADHD-specific altered functional connectivity was repeatedly found in the ventromedial prefrontal cortex, orbitofrontal cortex, frontal pole, amygdala, and ventral striatum (Bos et al., 2017; Costa Dias et al., 2013; Ho et al., 2015; Lin et al., 2014; Posner et al., 2013; L. Wang et al., 2009). Also, it was shown that differences in default mode network connectivity are associated with persistent ADHD outcomes (Mattfeld et al., 2014; Sudre et al., 2017). However, respective findings were derived from cross-sectional analyses and provide little insight into associations between changes in ADHD and preceding brain activity. Neither can they directly capture change at the individual level, nor can they directly related those changes to additional baseline factors (Kievit et al., 2018).

The node-specific analysis revealed a significant positive relationship between nodal efficiency at baseline and the course of ADHD severity for the right orbitofrontal cortex. Higher nodal efficiency values were associated with more favorable changes in ADHD severity over time. The present results extend literature that linked altered orbitofrontal cortex activation during cognitive control to persistent ADHD (Schulz et al., 2017). While also being thought to be influenced by cognitive processes (Rolls, 2019), the orbitofrontal cortex is particularly linked to the extinction or reevaluation of emotion processing. Similar to the ventromedial prefrontal cortex, the orbitofrontal cortex is considered essential for integrating information to allow emotional processes to be affected by goals, motivational states, or experiences. In primarily implicit processes, it provides contextual information, and thus helps to confine emotions to an appropriate range (Braunstein et al., 2017). For instance, it has been suggested that altered functional connections between the amygdala and the orbitofrontal cortex, which are particularly relevant for emotional outcome evaluation, may lie at the core of emotion network dysregulation in ADHD (Christiansen et al., 2019). The present re-

sults suggest that the course of ADHD severity depends on the efficiency with which the orbitofrontal cortex is functionally integrated with regions associated with emotion processing and implicit emotion regulation. Beyond this, they suggest that functional connectivity alterations relevant for the course of ADHD severity extend beyond regions commonly associated with cognitive control. In sum, nodal efficiency and thus the strength of integration of the orbitofrontal cortex with other regions involved in emotion processing and implicit regulation appear to have a positive impact on future changes in ADHD severity.

Contrary to our expectations, emotion dysregulation at baseline was not significantly correlated with nodal efficiency at baseline. However, both the latent emotion dysregulation variable and nodal efficiency are merely approximations for the true underlying concept of "emotion dysregulation". Presumably they show a non-significant correlation since they cover only partly overlapping aspects. For example, regions of the brain associated with cognitive control of emotions, e.g. via cognitive reappraisal, were not taken into account in the definition of the present emotion network. With respect to the orbitofrontal cortex, other variables associated with emotions, such as reward and motivation, may be more strongly correlated with nodal efficiency (Braunstein et al., 2017).

It is noticeable that both latent change score models that analyzed nodal efficiency showed significant effects in different ranges of network density. While the principal component-based model, which analyzed nodal efficiency of the whole network, revealed significant effects in the low to medium range of densities, the model investigating orbitofrontal nodal efficiency yielded significant results at the high end of density ranges (see Figs. 2D and 3D). Thus, for the former model, particularly strong functional connectivity between nodes seems to drive the significant relationship between the observed pattern of nodal efficiencies and change in ADHD severity, whereas for the latter model, medium-strong functional connectivity between the orbitofrontal cortex and the other nodes of the network appears to be most relevant. Following the approach of Ginestet et al. (2011) we applied density thresholding to separate effects of network topology from differences in functional connectivity strength. However, in some cases, density thresholding can bias the correlation between efficiency and external variables. Possibly, interindividual differences in efficiency are associated with individual differences in functional connectivity and subjects with low values in mean functional connectivity might be more affected by noisy, spurious connections (van den Heuvel et al., 2017). However, for both change score models the correlation between individual efficiency scores and mean functional connectivity values were not significant (BLCS model after PCA: $r = 0.077$, p=.443; BLCS model with orbitofrontal cortex: $r = 0.086$, p=.399). Thus, we found no evidence that interindividual differences in spurious connections influenced our results.

BLCS models provided an elegant method for studying change and the effect of behavioral and neural covariates on this change (Kievit et al., 2018). Although our sample was relatively large compared to other neuroimaging studies, nevertheless, for BLCS models the number of individuals used was rather low (Wolf et al., 2013). Yet, we were able to validate the robustness of the findings by conducting the analyses with an alternative parcellation scheme.

In the present analysis, emotion dysregulation was gauged from questionnaire subscales for conduct problems, emotional problems and emotional lability. Thus, it also entailed information strongly associated with other psychiatric disorders like depression, anxiety or conduct disorder (Vugteveen et al., 2021). While a relatively high proportion of individuals with corresponding comorbidities can be expected in the general ADHD population (Biederman, Newcorn, & Sprich, 1991), only few subjects showed these comorbidities in the present sample. Accordingly, it is rather unlikely that the results presented here are driven by comorbidities such as depression or anxiety.

We examined if emotion dysregulation and nodal efficiency of regions associated with emotion processing and implicit emotion regulation predicted change in ADHD severity from late adolescence into early adulthood. A pattern of low nodal efficiency in cortical brain regions associated with emotion processing and high nodal efficiency in subcortical regions and cortical region of implicit emotion regulation predicted a less severe course of ADHD. Further, we showed that higher nodal efficiency of the right orbitofrontal cortex was related to a more favorable course of ADHD. Moreover, emotion dysregulation, gauged as a latent variable from emotion problems, conduct problems and emotional lability captured from questionnaires was associated with more severe ADHD courses. Our study thus supports the involvement of emotion dysregulation and brain regions associated with emotion processing and implicit emotion regulation in the course of ADHD. Knowing that individuals with emotion regulation problems are at higher risk for a negative progression of ADHD, such individuals should receive special attention and additional interventions.

Credit author statement

Tammo Viering: Conceptualization, Methodology, Software, Formal Analysis, Writing – Original Draft, Visualization; **Pieter J. Hoekstra:** Conceptualization, Resources, Writing – Review & Editing, Project administration, Funding acquisition; **Alexandra Philipsen:** Writing – Review & Editing; **Jilly Naaijen:** Investigation, Writing – Review & Editing; **Andrea Dietrich:** Writing – Review & Editing; **Catharina A. Hartman:** Writing – Review & Editing; **Barbara Franke:** Writing – Review & Editing; **Jan K. Buitelaar:** Resources, Writing – Review & Editing, Project administration; Funding acquisition; **Andrea Hildebrandt:** Methodology, Formal Analysis, Writing – Review & Editing; **Christiane M. Thiel:** Conceptualization, Methodology, Resources, Writing – Review & Editing, Project administration, Funding acquisition; **Carsten Gießing:** Conceptualization, Methodology, Writing – Review & Editing

Declaration of Competing Interests

Jan K. Buitelaar has been in the past 3 years a consultant to / member of advisory board of / and/or speaker for Shire, Roche, Medice, and Servier. He is not an employee of any of these companies, and not a stock shareholder of any of these companies. He has no other financial or material support, including expert testimony, patents, royalties. Dr Philipsen has been in the last year a member of advisory board and a speaker for Shire/Takeda, and Medice. She received travel support from Janssen-Cilag, Shire/Takeda. She is an author of books and articles on ADHD published by Elsevier, Hogrefe, Schattauer, Kohlhammer, Karger, and Oxford publishers. No other disclosures were reported.

Data and code availability statement

The data are stored at the Donders Institute for Cognitive Neuroimaging and are available upon request from the corresponding author. The data are not publicly available due to privacy or ethical restrictions. Further information about the NeuroIMAGE project may be requested via the project leader Jan K. Buitelaar. Code may be provided upon request from the corresponding author.

Acknowledgements

The NeuroIMAGE project was supported by NWO Large Investment grant 175.010.2007.010, ZonMw Addiction: Risk Behaviour and Dependency grant 31160209, NWO MaGW grant 433-09-242, NWO National Initiative Brain & Cognition grant 056-13-015 (all to Jan K. Buitelaar), and ZonMw Priority Medicines Kinderen 113202005 grant (to Pieter Hoekstra). Additional funding comes from the Radboud University Nijmegen Medical Center, University Medical Center Groningen and Accare, and VU University Amsterdam. Furthermore, funding was contributed by the European Union's Seventh Framework and Horizon 2020 Programmes under grant agreement no 603016 (MATRICS) and 728018 (Eat2beNICE). This work reflects only the authors' views and the European Union is not liable for any use that may be made of the infor-

mation contained herein. Tammo Viering is funded by the Oldenburg-Groningen Joint Graduate Research Training Group “Translational Research: From Pathological Mechanisms to Therapy”. Jilly Naaijen is funded by a NWO VENI grant.

Supplementary materials

Supplementary material associated with this article can be found, in the online version, at doi:10.1016/j.neuroimage.2021.118729.

References

Achard, S., Bullmore, E., 2007. Efficiency and cost of economical brain functional networks. PLoS Comput. Biol. 3 (2), e17. doi:10.1371/journal.pcbi.0030017.

Baltes, P.B., Reese, H.W., Nesselroade, J.R., 1988. Life-Span Developmental Psychology : Introduction to Research Methods. Lawrence Erlbaum Associates.

Benjamini, Y., Hochberg, Y., 1995. Controlling the false discovery rate: a practical and powerful approach to multiple testing. J. R. Stat. Soc.: Ser. B (Methodol.) 57 (1), 289–300. doi:10.1111/j.2517-6161.1995.tb02031.x.

Biederman, J., Petty, C.R., Clarke, A., Lomedico, A., Faraone, S.V., 2011. Predictors of persistent ADHD: an 11-year follow-up study. J. Psychiatr. Res. 45 (2), 150–155. doi:10.1016/J.JPSYCHIRES.2010.06.009.

Bos, D.J., Oranje, B., Achterberg, M., Vlaskamp, C., Ambrosino, S., de Reus, M.A., Durston, S., 2017. Structural and functional connectivity in children and adolescents with and without attention deficit/hyperactivity disorder. J. Child Psychol. Psychiatry 58 (7), 810–818. doi:10.1111/jcpp.12712.

Braunstein, L.M., Gross, J.J., Ochsner, K.N., 2017. Explicit and implicit emotion regulation: a multi-level framework. Soc. Cogn. Affect. Neurosci. 12 (10), 1545–1557. doi:10.1093/scan/nsx096.

Brotman, M.A., Rich, B.A., Guyer, A.E., Lunsford, J.R., Horsey, S.E., Reising, M.M., Leibenluft, E., 2010. Amygdala activation during emotion processing of neutral faces in children with severe mood dysregulation versus ADHD or bipolar disorder. Am. J. Psychiatry 167 (1), 61–69. doi:10.1176/appi.ajp.2009.09010043.

Bunford, N., Evans, S.W., Wymbs, F., 2015. ADHD and emotion dysregulation among children and adolescents. Clin. Child Fam. Psychol. Rev. 18 (3), 185–217. doi:10.1007/s10567-015-0187-5.

Cai, L., Wei, X., Liu, J., Zhu, L., Wang, J., Deng, B., Wang, R., 2020. Functional integration and segregation in multiplex brain networks for Alzheimer’s disease. Front. Neurosci. 14. doi:10.3389/FNINS.2020.00051.

Caye, A., Spadini, A.V., Karam, R.G., Grevet, E.H., Rovaris, D.L., Bau, C.H., Kieling, C., 2016. Predictors of persistence of ADHD into adulthood: a systematic review of the literature and meta-analysis. Eur. Child Adolesc. Psychiatry (11) 25. doi:10.1007/S00787-016-0831-8.

Chen, Y., Huang, X., Wu, M., Li, K., Hu, X., Jiang, P., Gong, Q., 2019. Disrupted brain functional networks in drug-naïve children with attention deficit hyperactivity disorder assessed using graph theory analysis. Hum. Brain Mapp. 40 (17), 4877–4887. doi:10.1002/hbm.24743.

Christiansen, H., Hirsch, O., Albrecht, B., Chavanon, M.-.L., 2019. Attention-deficit/hyperactivity disorder (ADHD) and emotion regulation over the life span. Curr. Psychiatry Rep. 21 (3), 17. doi:10.1007/s11920-019-1003-6.

Conners, C.K., Erhardt, D., Epstein, J.N., Parker, J.D.A., Sitarenios, G., Sparrow, E., 1999. Self-ratings of ADHD symptoms in adults I: factor structure and normative data. J. Atten. Disord. 3 (3), 141–151. doi:10.1177/108705479900300303.

Conners, C.K., Sitarenios, G., Parker, J.D.A., Epstein, J.N., 1998a. The revised Conners’ parent rating scale (CPRS-R): factor structure, reliability, and criterion validity. J. Abnorm. Child Psychol. 26 (4), 257–268. doi:10.1023/A:1022602400621.

Conners, C.K., Sitarenios, G., Parker, J.D., Epstein, J.N., 1998b. Revision and restandardization of the Conners teacher rating scale (CTRS-R): factor structure, reliability, and criterion validity. J. Abnorm. Child Psychol. 26 (4), 279–291. Retrieved from http://www.ncbi.nlm.nih.gov/pubmed/9700520 .

Costa Dias, T.G., Wilson, V.B., Bathula, D.R., Iyer, S.P., Mills, K.L., Thurlow, B.L., Fair, D.A, 2013. Reward circuit connectivity relates to delay discounting in children with attention-deficit/hyperactivity disorder. Eur. Neuropsychopharmacol. 23 (1), 33–45. doi:10.1016/j.euroneuro.2012.10.015.

Devlieger, I., Mayer, A., Rosseel, Y., 2016. Hypothesis testing using factor score regression: a comparison of four methods. Educ. Psychol. Meas. (5) 76. doi:10.1177/0013164415607618.

Duan, K., Chen, J., Calhoun, V.D., Lin, D., Jiang, W., Franke, B., Liu, J., 2018. Neural correlates of cognitive function and symptoms in attention-deficit/hyperactivity disorder in adults. Neuroimage Clin. 19, 374–383. doi:10.1016/j.nicl.2018.04.035.

Etkin, A., Büchel, C., Gross, J.J., 2015. The neural bases of emotion regulation. Nat. Rev. Neurosci. 16 (11), 693–700. doi:10.1038/nrn4044.

Fan, L., Li, H., Zhuo, J., Zhang, Y., Wang, J., Chen, L., Jiang, T., 2016. The human brainnetome atlas: a new brain atlas based on connectional architecture. Cereb. Cortex 26 (8), 3508–3526. doi:10.1093/cercor/bhw157.

Finn, E.S., Shen, X., Scheinost, D., Rosenberg, M.D., Huang, J., Chun, M.M., Constable, R.T., 2015. Functional connectome fingerprinting: identifying individuals using patterns of brain connectivity. Nat. Neurosci. 18 (11), 1664–1671. doi:10.1038/nn.4135.

Francx, W., Oldehinkel, M., Oosterlaan, J., Heslenfeld, D., Hartman, C.A., Hoekstra, P.J., Mennes, M., 2015. The executive control network and symptomatic improvement in attention-deficit/hyperactivity disorder. Cortex 73, 62–72. doi:10.1016/J.CORTEX.2015.08.012.

Ginestet, C.E., Nichols, T.E., Bullmore, E.T., Simmons, A., 2011. Brain network analysis: separating cost from topology using cost-integration. PLoS ONE 6 (7), e21570. doi:10.1371/journal.pone.0021570.

Hagberg, A., Schult, D.A., Swart, P.J., 2008. Exploring Network Structure, Dynamics, and Function using NetworkX Retrieved from https://www.semanticscholar.org/paper/Exploring-Network-Structure%2C-Dynamics%2C-and-Function-Hagberg-Schult/06214a0cf38875da38586e81539890f7ad8aeb1c.

Hallquist, M.N., Hillary, F.G., 2019. Graph theory approaches to functional network organization in brain disorders: a critique for a brave new small-world. Netw. Neurosc. 3 (1), 1–26. doi:10.1162/netn_a_00054.

Herpertz, S.C., Huebner, T., Marx, I., Vloet, T.D., Fink, G.R., Stoecker, T., Herpertz-Dahlmann, B., 2008. Emotional processing in male adolescents with childhood-onset conduct disorder. J. Child Psychol. Psychiatry 49 (7), 781–791. doi:10.1111/j.1469-7610.2008.01905.x.

Ho, N.-.F., Chong, J.S.X., Koh, H.L., Koukouna, E., Lee, T.-.S., Fung, D., Zhou, J., 2015. Intrinsic affective network is impaired in children with attention-deficit/hyperactivity disorder. PLoS ONE 10 (9), e0139018. doi:10.1371/journal.pone.0139018.

Hoogman, M., Muetzel, R., Guimaraes, J.P., Shumskaya, E., Mennes, M., Zwiers, M.P., Franke, B., 2019. Brain imaging of the cortex in ADHD: a coordinated analysis of large-scale clinical and population-based samples. Am. J. Psychiatry 176 (7), 531–542. doi:10.1176/appi.ajp.2019.18091033.

Hulvershorn, L.A., Mennes, M., Castellanos, F.X., Di Martino, A., Milham, M.P., Hummer, T.A., Roy, A.K., 2014. Abnormal amygdala functional connectivity associated with emotional lability in children with attention-deficit/hyperactivity disorder. J. Am. Acad. Child Adolesc. Psychiatry 53 (3), 351–361. doi:10.1016/j.jaac.2013.11.012, e1.

Jenkinson, M., Beckmann, C.F., Behrens, T.E.J., Woolrich, M.W., Smith, S.M., 2012. FSL - review. Neuroimage doi:10.1016/j.neuroimage.2011.09.015.

Kaufman, J., Birman, B., Brent, D., Rao, U., Flynn, C., Moreci, P., Ryan, N., 1997. Schedule for affective disorders and schizophrenia for school-age children-present and lifetime version (K-SADS-PL): initial reliability and validity data. J. Am. Acad. Child Adolesc. Psychiatry 36 (7), 980–988. doi:10.1097/00004583-199707000-00021.

Kievit, R.A., Brandmaier, A.M., Ziegler, G., van Harmelen, A.-.L., de Mooij, S.M.M., Moutoussis, M., Dolan, R.J., 2018. Developmental cognitive neuroscience using latent change score models: a tutorial and applications. Dev. Cogn. Neurosci. 33, 99–117. doi:10.1016/J.DCN.2017.11.007.

Lin, P., Sun, J., Yu, G., Wu, Y., Yang, Y., Liang, M., Liu, X., 2014. Global and local brain network reorganization in attention-deficit/hyperactivity disorder. Brain Imaging Behav. 8 (4), 558–569. doi:10.1007/s11682-013-9279-3.

Ma, X., Jiang, G., Fu, S., Fang, J., Wu, Y., Liu, M., Wang, T., 2018. Enhanced network efficiency of functional brain networks in primary insomnia patients. Front. Psychiatry 9. doi:10.3389/FPSYT.2018.00046.

Mardia, K.V., 1970. Measures of multivariate skewness and kurtosis with applications. Biometrika 57 (3), 519–530. doi:10.1093/biomet/57.3.519.

Materna, L., Wiesner, C.D., Shushakova, A., Trieloff, J., Weber, N., Engell, A., Ohrmann, P., 2019. Adult patients with ADHD differ from healthy controls in implicit, but not explicit, emotion regulation. J. Psychiatry Neurosci. : JPN 44 (5), 340–349. doi:10.1503/jpn.180139.

Mattfeld, A.T., Gabrieli, J.D.E., Biederman, J., Spencer, T., Brown, A., Kotte, A., Whitfield-Gabrieli, S., 2014. Brain differences between persistent and remitted attention deficit hyperactivity disorder. Brain 137 (9), 2423–2428. doi:10.1093/brain/awu137.

Miranda, A., Colomer, C., Fernández, M.I., Presentación, M.J., Roselló, B., 2015. Analysis of personal and family factors in the persistence of attention deficit hyperactivity disorder: results of a prospective follow-up study in childhood. PLoS ONE (5) 10. doi:10.1371/JOURNAL.PONE.0128325.

Pan, J., Zhan, L., Hu, C., Yang, J., Wang, C., Gu, L., Wu, X., 2018. Emotion regulation and complex brain networks: association between expressive suppression and efficiency in the Fronto-parietal network and default-mode network. Front. Hum. Neurosci. 12, 70. doi:10.3389/fnhum.2018.00070.

Polanczyk, G.V., Willcutt, E.G., Salum, G.A., Kieling, C., Rohde, L.A., 2014. ADHD prevalence estimates across three decades: an updated systematic review and meta-regression analysis. Int. J. Epidemiol. 43 (2), 434–442. doi:10.1093/ije/dyt261.

Posner, J., Maia, T.V., Fair, D., Peterson, B.S., Sonuga-Barke, E.J., Nagel, B.J., 2011. The attenuation of dysfunctional emotional processing with stimulant medication: an fMRI study of adolescents with ADHD. Psychiatry Res. 193 (3), 151–160. doi:10.1016/j.pscychresns.2011.02.005.

Posner, J., Park, C., Wang, Z., 2014. Connecting the dots: a review of resting connectivity mri studies in attention-deficit/hyperactivity disorder. Neuropsychol. Rev. 24 (1), 3–15. doi:10.1007/s11065-014-9251-z.

Posner, J., Rauh, V., Gruber, A., Gat, I., Wang, Z., Peterson, B.S., 2013. Dissociable attentional and affective circuits in medication-naïve children with attention-deficit/hyperactivity disorder. Psychiatry Res.: Neuroimaging 213 (1), 24–30. doi:10.1016/j.pscychresns.2013.01.004.

Pruim, R.H.R., Beckmann, C.F., Oldehinkel, M., Oosterlaan, J., Heslenfeld, D., Hartman, C.A., Mennes, M., 2019. An integrated analysis of neural network correlates of categorical and dimensional models of attention-deficit/hyperactivity disorder. Biol. Psychiatry: Cogn. Neurosci. Neuroimaging 4 (5), 472–483. doi:10.1016/j.bpsc.2018.11.014.

Pruim, R.H.R., Mennes, M., van Rooij, D., Llera, A., Buitelaar, J.K., Beckmann, C.F., 2015. ICA-AROMA: a robust ICA-based strategy for removing motion artifacts from fMRI data. Neuroimage 112, 267–277. doi:10.1016/J.NEUROIMAGE.2015.02.064.

Riley, A.W., Spiel, G., Coghill, D., Döpfner, M., Falissard, B., Lorenzo, M.J.ADORE Study Group, 2006. Factors related to health-related quality of life (HRQoL) among children with ADHD in Europe at entry into treatment. Eur. Child Adolesc. Psychiatry 15 (Suppl 1), I38–I45. doi:10.1007/s00787-006-1006-9.

Rocca, M.A., Valsasina, P., Meani, A., Falini, A., Comi, G., Filippi, M., 2016. Impaired functional integration in multiple sclerosis: a graph theory study. Brain Struct. Funct. 221 (1), 115–131. doi:10.1007/s00429-014-0896-4.

Rolls, E.T., 2019. The orbitofrontal cortex and emotion in health and disease, including depression. Neuropsychologia 128, 14–43. doi:10.1016/J.NEUROPSYCHOLOGIA.2017.09.021.

Rosseel, Y., 2012. lavaan: an R package for structural equation modelling. J. Stat. Softw. 48 (2), 1–36. doi:10.18637/jss.v048.i02.

Rubia, K., 2011. Cool" inferior frontostriatal dysfunction in attention-deficit/hyperactivity disorder versus "hot" ventromedial orbitofrontal-limbic dysfunction in conduct disorder: a review. Biol. Psychiatry 69 (12), e69–e87. doi:10.1016/J.BIOPSYCH.2010.09.023.

Rubia, K., 2018. Cognitive neuroscience of attention deficit hyperactivity disorder (ADHD) and its clinical translation. Front. Hum. Neurosci. 12, 100. doi:10.3389/fnhum.2018.00100.

Sasser, T.R., Kalvin, C.B., Bierman, K.L., 2016. Developmental trajectories of clinically significant ADHD symptoms from grade 3 through 12 in a high-risk sample: predictors and outcomes. J. Abnorm. Psychol. 125 (2), 207. doi:10.1037/ABN0000112.

Schermelleh-Engel, K., Moosbrugger, H., & Müller, H.H. (2003). *Evaluating the fit of structural equation models: tests of significance and descriptive goodness-of-fit measures*. Retrieved from https://www.semanticscholar.org/paper/Evaluating-the-fit-of-structural-equation-models%3A-Schermelleh-Engel-Moosbrugger/18d1b08b1cca0f0d6f8121281d6d16f986ac3f61

Schulz, K.P., Li, X., Clerkin, S.M., Fan, J., Berwid, O.G., Newcorn, J.H., Halperin, J.M., 2017. Prefrontal and parietal correlates of cognitive control related to the adult outcome of attention-deficit/hyperactivity disorder diagnosed in childhood. Cortex; J. Devot. Study Nervous Syst. Behav. 90. doi:10.1016/J.CORTEX.2017.01.019.

Shaw, P., Malek, M., Watson, B., Greenstein, D., De Rossi, P., Sharp, W., 2013. Trajectories of cerebral cortical development in childhood and adolescence and adult attention-deficit/hyperactivity disorder. Biol. Psychiatry 74 (8), 599–606. doi:10.1016/j.biopsych.2013.04.007.

Shaw, P., Stringaris, A., Nigg, J., Leibenluft, E., 2014. Emotion dysregulation in attention deficit hyperactivity disorder. Am. J. Psychiatry doi:10.1176/appi.ajp.2013.13070966.

Shaw, P., Sudre, G., 2021, January 15. Adolescent attention-deficit/hyperactivity disorder: understanding teenage symptom trajectories. Biol. Psychiatry 89, 152–161. doi:10.1016/j.biopsych.2020.06.004.

Shaw, P., Sudre, G., Wharton, A., Weingart, D., Sharp, W., Sarlls, J., 2015. White matter microstructure and the variable adult outcome of childhood attention deficit hyperactivity disorder. Neuropsychopharmacology 40 (3), 746–754. doi:10.1038/npp.2014.241.

Shen, X., Tokoglu, F., Papademetris, X., Constable, R.T., 2013. Groupwise whole-brain parcellation from resting-state fMRI data for network node identification. Neuroimage 82, 403–415. doi:10.1016/j.neuroimage.2013.05.081.

Shim, M., Im, C., Kim, Y., Lee, S., 2018. Altered cortical functional network in major depressive disorder: a resting-state electroencephalogram study. NeuroImage: Clin. 19, 1000–1007. doi:10.1016/J.NICL.2018.06.012.

Simões, E.N., Carvalho, A.L.N., Schmidt, S.L., 2017. What does handedness reveal about ADHD? An analysis based on CPT performance. Res. Dev. Disabil. 65, 46–56. doi:10.1016/j.ridd.2017.04.009.

Spencer, A.E., Marin, M.-F., Milad, M.R., Spencer, T.J., Bogucki, O.E., Pope, A.L., Biederman, J., 2017. Abnormal fear circuitry in Attention Deficit Hyperactivity Disorder: a controlled magnetic resonance imaging study. Psychiatry Res.: Neuroimaging 262, 55–62. doi:10.1016/J.PSCYCHRESNS.2016.12.015.

Sudre, G., Sharp, W., Kundzicz, P., Bouyssi-Kobar, M., Norman, L., Choudhury, S., Shaw, P., 2020. Predicting the course of ADHD symptoms through the integration of childhood genomic, neural, and cognitive features. Mol. Psychiatry 1–9. doi:10.1038/s41380-020-00941-x.

Sudre, G., Szekely, E., Sharp, W., Kasparek, S., Shaw, P., 2017. Multimodal mapping of the brain's functional connectivity and the adult outcome of attention deficit hyperactivity disorder. Proc. Natl. Acad. Sci. U.S.A. 114 (44), 11787–11792. doi:10.1073/pnas.1705229114.

Szekely, E., Sudre, G.P., Sharp, W., Leibenluft, E., Shaw, P., 2017. Defining the neural substrate of the adult outcome of childhood ADHD: a multimodal neuroimaging study of response inhibition. Am. J. Psychiatry 174 (9), 867–876. doi:10.1176/appi.ajp.2017.16111313.

Team, R. D. C., & R Development Core Team, R., 2016. R: A Language and Environment for Statistical Computing. R Foundation for Statistical Computing doi:10.1007/978-3-540-74686-7.

Uddin, L.Q., Nomi, J.S., Hébert-Seropian, B., Ghaziri, J., Boucher, O., 2017. Structure and function of the human insula. J. Clin. Neurophysiol. : Off. Publ. Am. Electroencephalograph. Soc. 34 (4), 300–306. doi:10.1097/WNP.0000000000000377.

van den Heuvel, M., de Lange, S., Zalesky, A., Seguin, C., Yeo, B., Schmidt, R., 2017. Proportional thresholding in resting-state fMRI functional connectivity networks and consequences for patient-control connectome studies: issues and recommendations. Neuroimage 152. doi:10.1016/J.NEUROIMAGE.2017.02.005.

van Widenfelt, B.M., Goedhart, A.W., Treffers, P.D.A., Goodman, R., 2003. Dutch version of the strengths and difficulties questionnaire (SDQ). Eur. Child Adolesc. Psychiatry 12 (6), 281–289. doi:10.1007/s00787-003-0341-3.

von Rhein, D., Mennes, M., van Ewijk, H., Groenman, A.P., Zwiers, M.P., Oosterlaan, J., Buitelaar, J., 2015. The NeuroImage study: a prospective phenotypic, cognitive, genetic and MRI study in children with attention-deficit/hyperactivity disorder. Design and descriptives. Eur. Child Adolesc. Psychiatry 24 (3), 265–281. doi:10.1007/s00787-014-0573-4.

Vugteveen, J., de Bildt, A., Theunissen, M., Reijneveld, M., Timmerman, M., 2021. Validity aspects of the strengths and difficulties questionnaire (SDQ) adolescent self-report and parent-report versions among Dutch adolescents. Assessment 28 (2), 601–616. doi:10.1177/1073191119858416.

Wang, L., Zhu, C., He, Y., Zang, Y., Cao, Q., Zhang, H., Wang, Y., 2009. Altered small-world brain functional networks in children with attention-deficit/hyperactivity disorder. Hum. Brain Mapp. 30 (2), 638–649. doi:10.1002/hbm.20530.

Wang, Y., Zhao, Y., Nie, H., Liu, C., Chen, J., 2018. Disrupted brain network efficiency and decreased functional connectivity in multi-sensory modality regions in male patients with alcohol use disorder. Front. Hum. Neurosci. 12. doi:10.3389/FNHUM.2018.00513.

Wehmeier, P.M., Schacht, A., Barkley, R.A., 2010. Social and emotional impairment in children and adolescents with ADHD and the impact on quality of life. J. Adolesc. Health : Off. Publ. Soc. Adolesc. Med. 46 (3). doi:10.1016/J.JADOHEALTH.2009.09.009.

Willcutt, E.G., 2012. The prevalence of DSM-IV attention-deficit/hyperactivity disorder: a meta-analytic review. Neurotherapeutics 9 (3), 490. doi:10.1007/S13311-012-0135-8.

Wolf, E.J., Harrington, K.M., Clark, S.L., Miller, M.W., 2013. Sample size requirements for structural equation models: an evaluation of power, bias, and solution propriety. Educ. Psychol. Meas. 76 (6), 913. doi:10.1177/0013164413495237.

Yu, X., Liu, L., Chen, W., Cao, Q., Zepf, F.D., Ji, G., Wang, Y., 2016. Integrity of amygdala subregion-based functional networks and emotional lability in drug-naïve boys with ADHD. J. Atten. Disord. doi:10.1177/1087054716661419, 108705471666141.

Yuan, K.-H., Zhong, X., 2013. Robustness of fit indices to outliers and leverage observations in structural equation modeling. Psychol. Methods 18 (2), 121–136. doi:10.1037/a0031604.